International Core Journal of Engineering Volume 12 Issue 5, 2026
ISSN: 2414-1895 DOI: 10.6919/ICJE.202605_12(5).0019

Dynamic Process Control based on an AI Model Cluster for Atmospheric and Vacuum Distillation

Jun Liu

Dalian West Pacific Petrochemical Co., Ltd., Dalian, China

Abstract

From November 2024 to August 2025, a data-driven real-time closed-loop optimization project was carried out for a 10 Mt/a atmospheric and vacuum distillation unit. The study was intended to address the strong coupling, frequent operating-mode switching, and limited long-term effectiveness of conventional optimization methods in large crude distillation systems. A process-oriented artificial intelligence (AI) model cluster was therefore developed by using full-process modular artificial neural networks (ANNs) to characterize the coupled states of the unit and reflect changes in operating conditions. On this basis, an intelligent execution system (iES) was built to translate plant-wide optimization results into dynamic control targets acceptable to the field, which were then implemented through multivariable advanced control schemes at the distributed control system (DCS) level. Industrial application shows that, within quality and safety boundaries, this method can transfer optimization solutions to the production unit in a safe and stable manner, demonstrating good industrial applicability.

Keywords

Atmospheric and Vacuum Distillation; Process AI Model Cluster; Dynamic Optimization; Intelligent Control System; Expert Knowledge.

1. Introduction

Atmospheric and vacuum distillation is the starting point of the refinery process, and its operating condition directly affects downstream unit loading, product cut distribution, and the overall energy consumption of the refinery. In practice, changes in crude properties, throughput adjustments, and performance degradation of equipment often occur simultaneously. The unit therefore exhibits strong coupling, time-varying behavior, and multiple constraints. Under such conditions, it is difficult to maintain a reasonable balance among yield, product quality, and energy consumption over long operating periods by relying only on operator experience or conventional DCS control.

In recent years, model predictive control (MPC), real-time optimization (RTO), digital twins, and data-driven soft sensing have developed rapidly in the process industry, while the coordinated management of plant-wide operations under Industry 4.0 paradigms has also received increasing attention [1]. For a 10-Mt/a crude distillation unit, however, the key difficulty often lies less in calculating an optimum than in extracting from the upper-layer optimization results a set of decisions that can be executed continuously by multiple DCS controllers while locking product quality and safety boundaries online [2, 3, 4, 5, 6, 7, 8].

Using the Dalian West Pacific 10-Mt/a atmospheric and vacuum distillation unit as a case study under the project “Data-Driven Real-Time Closed-Loop Optimization Method for Atmospheric and Vacuum Distillation,” this paper analyzes three aspects: construction of the process AI model cluster, development of the iES execution layer, and field closed-loop testing. Two specific issues are discussed: (1) how a dual-protection mechanism combining quality prediction/early warning with

ISSN: 2414-1895 DOI: 10.6919/ICJE.202605_12(5).0019

hard-boundary interlocks can be used during execution, and (2) how the strategy of "small steps with quick iteration" can be used to transform plant-wide optimization targets into trackable and convergent field operating paths.

2. Architecture of the Data-Driven Real-Time Closed-Loop Optimization Method

The real-time closed-loop optimization method is organized into four functional layers. Each layer has a clear role, while the layers remain tightly connected. The bottom layer carries out data processing and steady-state identification; the middle layer performs logical-model calculation and optimization solving; the upper layer handles execution scheduling and closed-loop feedback. Together, they form a closed process of "data processing–model calculation–optimization solving–actual execution."

(1) Data and steady-state analysis layer

The system integrates DCS databases, laboratory information management system (LIMS) data, and manufacturing execution system (MES) data. The raw data are cleaned, time-aligned, filtered, and screened for abnormal points, yielding 2.681 billion valid records. To address short-term fluctuations, abnormal behaviors, and non-steady segments observed in the field, a combined method of multi-level steady-state screening and fluctuation-threshold judgment is used to extract valid samples. Meanwhile, 26 variables, including the initial column overhead temperature, furnace outlet temperature, atmospheric tower overhead pressure, and main-column draw temperatures, are selected to construct a steady-state index. Once the overall index indicates a deviation, model reconstruction and correction are triggered.

(2) Process AI model cluster layer

Historical plant data do not provide sufficient coverage of boundary conditions, switching conditions, or rare operating scenarios. The project therefore started from thousands of representative operating-condition samples mined from the field, supplemented them with samples generated by first-principles models, and then used a cloud platform to create expanded operating scenarios. This process ultimately produced about 3 million expanded-condition samples, 50 billion enhanced data records, and a variable domain involving 18,727 variables. Here, data enhancement is not merely an expansion of sample quantity; it is intended to compensate for those operating regions that are least represented in historical data and most sensitive to optimization and control.

The process AI model cluster contains nearly one thousand ANN sub-models. Model training follows a cyclic workflow of "sample composition–model training–result validation–data enhancement–retraining." A typical ANN includes input, hidden, and output layers. Basic process variables, disturbance variables, and state variables are used as inputs to predict key qualities and operating outcomes. Complex relationships are represented through weights, biases, and nonlinear activation functions, and the regression-training process continuously updates the weights and biases so that the ANN outputs approach the actual process response as closely as possible [6, 9]. Compared with a single model, the clustered modeling approach is better suited to representing the interactions among the tower system, furnaces, and heat-exchange network in the atmospheric and vacuum distillation unit.

(3) Global real-time optimization layer

The global real-time optimization layer uses the process AI model cluster as its computational core. Under given business objectives, price information, quality specifications, and process boundary conditions, it performs plant-wide optimization of the initial column, atmospheric tower, vacuum tower, atmospheric furnaces, vacuum furnace, and heat exchange network, involving 52 optimization variables in total [10].

(4) iES intelligent execution layer

ISSN: 2414-1895 DOI: 10.6919/ICJE.202605_12(5).0019

The iES layer receives the execution results generated by global optimization and converts them into dynamic control targets that can be issued to the field and tracked during implementation. According to the predefined execution sequence, step size, and waiting time, the system writes new actions into multiple multivariable MPC controllers, and then adjusts the direction and magnitude of subsequent actions dynamically based on the field execution feedback. In this way, operating fluctuations during execution are minimized and product-quality excursions are reduced. The soft sensors required for execution are also derived from the process AI model cluster, enabling real-time estimation of key crude and sidestream product properties and thereby providing quality feedback for dynamic control. In field application, the execution after a single round of optimization can basically be completed within about 0.5 h, and the dynamic deviation of the main optimization variables can be controlled within 0.5 °C [4, 5, 7].

3. Design and Implementation of the iES Intelligent Control System

3.1 Background and Positioning of the System Design

In atmospheric and vacuum distillation units, DCS loops are first responsible for basic stabilizing control, while MPC further guarantees constrained multivariable coordination. For a 10-Mt/a unit, however, a single local controller is insufficient. A large number of cross-unit couplings cannot be fully included in one control loop, and product quality can only be adjusted indirectly through variables such as temperatures that influence many other process states. In addition, the parameters of process models gradually drift and become mismatched as operating conditions and equipment states change [7, 9, 11].

For this reason, iES is defined in this study as the execution-coordination layer of the process digital twin system. It does not replace MPC. Its role is to connect upper-layer optimization with lower-layer control: on the one hand, it decomposes plant-level optimization solutions into target values and constraints acceptable to each controller; on the other hand, it coordinates constraint verification, step-size determination, and feedback correction during execution. Through quality pre-judgment and early warning, hard-boundary interlocks, and stepwise advancement, iES transforms “the best solution calculated by optimization” into “the best solution that can be implemented robustly in the field.”

3.2 Core Operating Mechanism

The essence of iES lies in decomposing the target state produced by global optimization into a sequence of operating instructions that can be executed step by step by field control devices, thereby forming a closed loop covering state perception, analysis, model-based optimization, optimization decision-making, control execution, and result feedback. The iES system mainly consists of two parts: intelligent optimization and intelligent control. Intelligent optimization performs steady-state recognition, digital-twin visualization, and optimization-scheme solving, whereas intelligent control transfers optimization results to DCS-side controllers for execution. The execution layer covers multiple unit controllers, including single loops, sidestream quality constraints, the heat-exchange network, atmospheric furnaces, the initial-column–atmospheric-tower section, the vacuum furnace, and the vacuum tower. These unit controllers operate under a common iES target framework, adjust control instructions in a rolling manner according to field-controller feedback, and rely on the process digital twin to estimate quality changes in real time, so that the unit gradually converges to a new steady state [4, 5, 7, 8].

In actual operation, iES does not pull all variables directly to their target positions in a single action. Instead, it adopts a strategy of “small steps with quick iteration.” A single-step movement and an upper limit are defined for each variable. After every step, the soft-sensor prediction is compared with the field response. If the deviation becomes larger, the next step is tightened automatically; when necessary, some variable movements are even suspended, and model parameters are adjusted according to gain analysis results. This mechanism allows the controller to follow the process evolution and avoids excessive actions that might introduce new oscillations.

ISSN: 2414-1895 DOI: 10.6919/ICJE.202605_12(5).0019

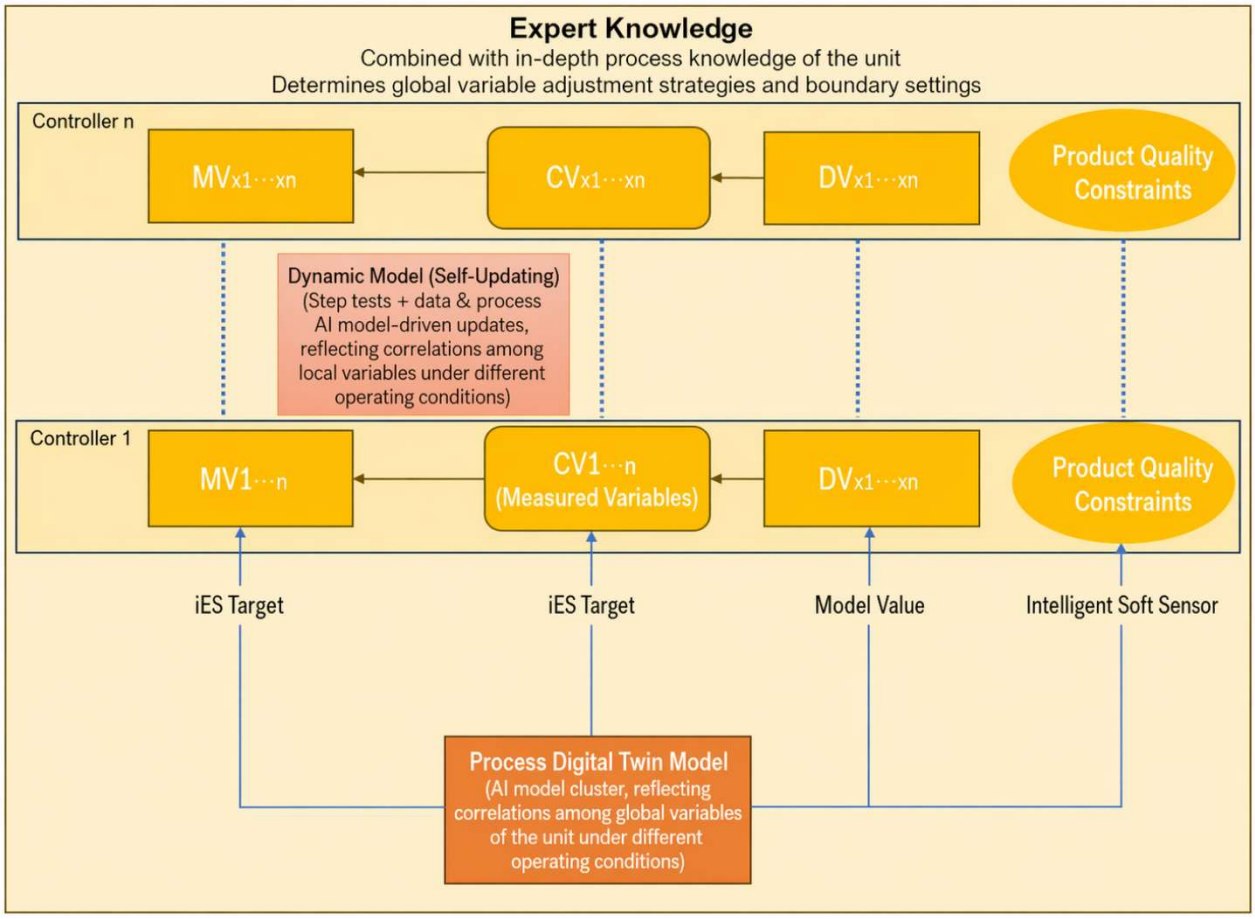

Figure 1. Core operating mechanism of iES

As shown in Figure 1, iES operates on the basis of a unified coupling and quality-calculation platform provided by the process AI model cluster. Through a "prediction–verification–feedback" mechanism, plant-wide optimization targets are converted into continuous action sequences that can be executed by multiple controllers, allowing the unit to move progressively toward the target operating condition.

3.3 Key Engineering Design and Implementation Strategies

3.3.1. Controller-variable Design based on Global Gain Analysis

In this project, the intelligent optimization system was deployed on the operator workstation in the central control room, while the iES intelligent control system was deployed on the DCS side. For the main process sections of the atmospheric and vacuum distillation unit, modules were defined for sidestream quality constraints and destinations, single-loop optimization variables, the heat-exchange network, atmospheric furnace F01A, atmospheric furnace F01B, the initial-column–atmospheric-tower section, vacuum furnace F02, and the vacuum tower. The control loops were not configured by mechanically applying a standard template. Instead, material flows, energy-transfer paths, and interaction relationships among units, equipment, and loops were first analyzed, after which the control structure and logic were reconstructed in combination with field operators' experience and process understanding. The manipulated variables (MVs), controlled variables (CVs), and disturbance variables (DVs) were then determined accordingly. Taking the initial-column–atmospheric-tower section as an example, the project team reselected manipulated and disturbance variables on the basis of clarified process causal chains, so that the pairing between controlled objects and the variables that are actually more sensitive in plant operation was consistent with field reality.

ISSN: 2414-1895 DOI: 10.6919/ICJE.202605_12(5).0019

Under a conventional design scheme, the main-column draw temperature of the first atmospheric sidestream is regulated by the first-sidestream flow rate and the atmospheric overhead circulating reflux. Based on many years of operating experience, however, the project team judged that the atmospheric tower top reflux has a stronger and more direct influence on this temperature. The engineering scheme therefore increased the gain associated with atmospheric top reflux so as to strengthen the quality control of the aviation-kerosene cut from the first atmospheric sidestream. This is because tower-top reflux directly affects mass transfer and heat transfer in the upper section of the tower and continuously alters the concentration distribution and phase equilibrium of light and heavy components in the region of the first sidestream. By contrast, overhead circulating reflux mainly reflects local heat removal, and its influence on lower cut positions is relatively limited. According to plant operating data and gain-analysis results, the coupling between the first atmospheric sidestream main-column draw temperature and top reflux is stronger than that between this temperature and overhead circulating reflux; therefore, the former is more suitable as a control-related variable in this unit.

In another example, the setpoint of the first atmospheric sidestream flow can be used to regulate the main-column draw temperature of that sidestream, but changes in this flow also affect the main-column draw temperature of the second atmospheric sidestream. To account for this coupling, the project team introduced the setpoint of the first atmospheric sidestream flow into the disturbance term of the control-object model for the second atmospheric sidestream temperature, thereby improving the controller's ability to identify and compensate for actual disturbances.

Table 1. Examples of variable settings for selected controllers

Optimization variable	**Manipulated variable**		**Disturbance variable**
Main-column draw temperature of the 1st atmospheric sidestream	Setpoint of 1st atmospheric sidestream flow	Setpoint of atmospheric tower top reflux	Flow of atmospheric 1st middle sidestream
Main-column draw temperature of the 2nd atmospheric sidestream	Setpoint of 2nd atmospheric sidestream flow	Setpoint of return-to-tower flow from atmospheric 1st middle sidestream	Setpoint of 1st atmospheric sidestream flow

3.3.2. Dual-layer Closed-loop Constraints for Quality and Safety

Quality and safety are the two bottom lines that cannot be crossed in closed-loop optimization. Accordingly, the iES execution layer was designed with two lines of defense: "soft-constraint prediction and early warning" and "hard-constraint logic interlock." The former intervenes before a risk develops into an actual limit violation, while the latter serves as the final rigid safeguard immediately before any action crosses the feasible operating region, thereby keeping the unit within an acceptable range at all times.

(1) Soft constraints: AI-model-based prediction and early warning of quality excursions. At the soft-constraint layer, soft sensors from the process AI model cluster are used to predict key quality indicators such as sidestream distillation range and flash point on a minute-by-minute rolling basis. The system therefore evaluates whether a candidate action is likely to cause a quality violation. If the soft-sensor results diverge from laboratory analyses, the model is re-identified or its parameters are fine-tuned to maintain quality predictability [3,6, 7, 12].

(2) Hard constraints: DCS logic interlocks and rigid safety-boundary protection. In the hard-constraint layer, the upper and lower limits of process-parameter optimization are linked directly to DCS alarm limits, interlock limits, and empirically acceptable operating ranges. This means that although the global optimizer may move closer to extreme conditions, the execution layer must first satisfy the hard-boundary requirements so that actual actions remain within the allowable safety range.

ISSN: 2414-1895 DOI: 10.6919/ICJE.202605_12(5).0019

(3) Coordination between soft and hard constraints under the "small-steps" strategy. These two protections do not operate independently. They are integrated with the "small steps with quick iteration" strategy. On the basis of AI predictions, the system first adjusts the step size and sequence with relatively loose early-warning logic, and then performs hard-boundary checks on candidate actions. After each step, the strictness of constraints and the next step size are updated according to the reverse deviation, forming a two-layer safeguard that reduces the chance of boundary approach and prevents actual boundary crossing.

For example, to ensure equipment safety, product quality, and the normal efficiency of the first atmospheric sidestream stripper, the project team established a coupling relationship in the initial-column–atmospheric-tower controller between the liquid-level protection of the first atmospheric sidestream stripper and the flow in branch 2 of the return stream from the atmospheric second middle sidestream. When the liquid level of the first atmospheric sidestream stripper falls below the lower limit plus 5%, the flow in this return branch is gradually reduced to its lower limit so as to slow the decrease in liquid level.

In field implementation, the initial protection limits for the liquid level of the first atmospheric sidestream stripper were set at 80%–100%, and the flow of branch 2 of the return stream from the atmospheric second middle sidestream was controlled at 195–205 t/h. After the lower limit of liquid-level protection was raised to 90%, the actual liquid level was 91.92%, which was still below the lower-limit-plus-5% threshold (95%). The system therefore automatically reduced the relevant steady-state flow value gradually to its lower limit, and the entire adjustment process took about 3 min.

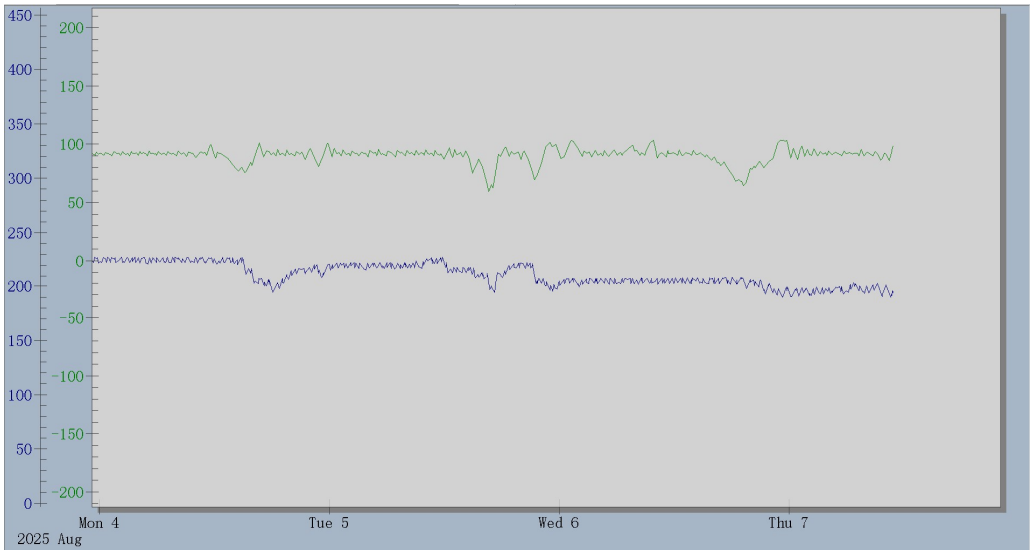

Figure 2. Coupling between the liquid-level protection of the 1st atmospheric sidestream stripper and the flow in branch 2 of the return stream from the atmospheric 2nd middle sidestream

Using the same idea, the project team added liquid-level protection for the first vacuum sidestream in the vacuum-tower controller. When the liquid level of the first vacuum sidestream falls below the lower limit plus 5%, the external flow of this sidestream is gradually restricted to its lower limit to suppress the downward trend of the liquid level.

3.3.3. Parameterized Implementation of the Adaptive "Small-step" Strategy

To balance response speed and execution smoothness, iES adopts a parameterized version of the "small steps with quick iteration" strategy. The variable changes calculated by upper-layer optimization are not sent to the controlled unit all at once; instead, they are decomposed into several adjustable step lengths. During execution, the deviation between the optimization prediction and the current field response is continuously evaluated. When the deviation increases significantly, the next

ISSN: 2414-1895 DOI: 10.6919/ICJE.202605_12(5).0019

execution step is reduced to avoid overshoot and oscillation. Each round realizes only the currently optimal step, and the next step is recalculated using the latest measurements. In this rolling way, the system moves toward the optimum point step by step while maintaining stable plant operation.

3.4 Industrial Application Test and Effect Analysis

3.4.1. Overview of the Application Test

On July 14, 2025, under stable operating conditions, the project team carried out a closed-loop test on the vacuum section of the unit. Before the test, the ranges of sidestream draw temperature, sidestream flow, and the intermediate vacuum-section flow were specified. In addition, according to price requirements, the vacuum overhead and the first vacuum sidestream were both designated as relatively high-value diesel fractions. The test was intended to determine whether the system could automatically optimize the operation under these constraints and increase the output of the first vacuum sidestream, thereby revealing the optimization direction and execution behavior. The vacuum-tower controller was activated at 9:00 a.m., iES optimization was enabled at 9:10 a.m., and the rolling execution commands were issued from 9:34 a.m. to 12:34 p.m., for a total of six rounds.

3.4.2. Statistical Analysis

(1) Comparison of current values before and after adjustment. After several optimization schemes had been implemented, the outlet temperature of vacuum furnace F02 increased from 351.0 °C to 353.51 °C. The draw temperatures of the first, second, and third vacuum sidestreams increased by 4.83 °C, 2.86 °C, and 2.84 °C, respectively. The intermediate flow rates decreased to different extents, while the flow rates of the first, second, and third vacuum sidestreams increased by 4.21 t/h, 2.55 t/h, and 1.01 t/h, respectively. The overall trend is consistent with the objective of increasing vacuum diesel production.

Table 2. Comparison of current values for increasing vacuum diesel production

Tag	Description	Unit	9:00	10:20	10:50	11:50	13:26	Optimization Increment
TIR1602	1st vacuum sidestream draw temperature	°C	92.5	95.07	95.44	96.01	97.33	4.83
TIR1603	2nd vacuum sidestream draw temperature	°C	209.38	210.36	210.59	211.41	212.24	2.86
TIR1604	3rd vacuum sidestream draw temperature	°C	272.87	273.43	273.55	273.90	275.71	2.84
FIC1601	1st vacuum middle flow setpoint	t/h	150.43	145.37	146.04	154.48	149.29	-1.14
FIC1602	2nd vacuum middle flow setpoint	t/h	240.14	242.24	241.38	230.69	237.28	-2.86
FIC1603	3rd vacuum middle flow setpoint	t/h	367.20	367.14	368.15	368.93	360.81	-6.39
FICQ1601	1st vacuum sidestream flow setpoint	t/h	17.07	20.91	20.38	19.99	21.28	4.21
FICQ1602	2nd vacuum sidestream flow setpoint	t/h	130.15	129.99	130.57	130.74	132.70	2.55
FICQ1603	3rd vacuum sidestream flow setpoint	t/h	17.09	17.72	17.72	17.88	18.10	1.01

ISSN: 2414-1895 DOI: 10.6919/ICJE.202605_12(5).0019

(2) Comparison of steady-state values before and after adjustment. The steady-state comparison further shows that the optimization effect is consistent with the target of increasing vacuum diesel output.

Table 3. Comparison of steady-state values for increasing vacuum diesel production

Tag	Description	Unit	9:00 Steady	13:26 Steady	Optimization Increment
TIR1602	1st vacuum sidestream draw temperature	°C	92.5	97.0	4.5
TIR1603	2nd vacuum sidestream draw temperature	°C	209.36	212.51	3.15
TIR1604	3rd vacuum sidestream draw temperature	°C	272.5	275.79	3.29
FIC1601	1st vacuum middle flow setpoint	t/h	152.94	150.42	-2.52
FIC1602	2nd vacuum middle flow setpoint	t/h	237.86	235.34	-2.52
FIC1603	3rd vacuum middle flow setpoint	t/h	372.71	368.41	-4.3
FICQ1601	1st vacuum sidestream flow setpoint	t/h	16.41	21.17	4.76
FICQ1602	2nd vacuum sidestream flow setpoint	t/h	131.0	132.0	1.0
FICQ1603	3rd vacuum sidestream flow setpoint	t/h	17.0	17.98	0.98

(3) Execution duration and accuracy of optimization variables. From the execution process, a single optimization scheme can usually be implemented within 0.5 h, and the one-time dynamic deviation of sidestream draw temperature is less than 0.5 °C.

(4) Field trend chart. Field trends show that after the vacuum section was operated with iES intelligent optimization, the liquid-level fluctuation of the first vacuum sidestream decreased significantly. This indicates that the vacuum section achieved increased sidestream production while also reducing plant operating fluctuations. Figure 3 shows the trend of the first vacuum sidestream flow.

Figure 3. Trend of the 1st vacuum sidestream flow

3.4.3. Discussion of Test Results

(1) Convergence speed: rapid stabilization under rolling execution. The system issued optimization schemes continuously in a rolling manner. Six rounds were generated from 9:34 to 12:34. Taking Scheme 2 as an example, after it was issued at 10:04, the optimization had basically reached a steady state by about 10:20, indicating that the stepwise strategy enabled the system to converge to a new operating condition rapidly and smoothly.

ISSN: 2414-1895 DOI: 10.6919/ICJE.202605_12(5).0019

(2) Execution accuracy: small deviation and stable target tracking. The test results show that the execution time for a scheme to take effect was less than 0.5 h, and the dynamic deviation of sidestream draw temperature was below 0.5 °C. This indicates that iES has relatively stable target-tracking capability through coordinated setpoint scheduling, controller coordination, and feedback correction.

(3) Mechanistic evidence: approaching the optimum within constraints, reflecting coordination and boundary management. As the scheme progressed step by step, optimization actions such as single-loop optimization of the F02 outlet temperature were continuously introduced, and the target sidestream was gradually shifted toward the higher-value direction. Eventually, within the allowable scheme range, the unit was operated close to the boundary, for example with the F02 outlet temperature maximized at 353.51 °C and the first vacuum sidestream flow maximized at 21.28 t/h. These results indirectly demonstrate the effectiveness of continuous multi-controller scheduling and boundary management.

4. Conclusion and Outlook

Engineering application shows that, for an atmospheric and vacuum distillation unit to realize closed-loop optimization, an upper-layer “plant brain” alone is not sufficient. An execution layer is also required to convert optimization results into stable and implementable plant actions. Based on unified target configuration, coordinated tuning strategies, and multi-level constraints, the iES intelligent control system translates optimization solutions from the process digital twin and AI model cluster into stepwise execution paths acceptable to the field. The results indicate that the dynamic process control method based on a process AI model cluster has already been applied to real-time closed-loop optimization of atmospheric and vacuum distillation units and has been verified in practice. Its performance, however, still depends on the quality of the underlying DCS basic control. If loop oscillation, valve hysteresis or stiction, and improper controller tuning exist in the field, the convergence speed and execution accuracy of iES are both affected, and the economic benefits of optimization are reduced accordingly.

Future work may include online assessment of loop health, so that loop oscillation, hysteresis, response time, and related characteristics can be incorporated into execution scheduling indices, thereby enabling further dynamic adaptation of step size, execution order, and variable priority.

References

[1] M. Vaccari, R. Bacci Di Capaci, E. Brunazzi, et al.: Optimally Managing Chemical Plant Operations: An Example Oriented by Industry 4.0 Paradigms, Industrial & Engineering Chemistry Research, Vol. 60 (2021) No. 21, p.7853-7867.

[2] Y.D. Su: Improvement and Optimization of Advanced Control for Crude Distillation Units, Petrochemical Automation, Vol. 59 (2023) No. 1.

[3] Y.D. Su: Application of Soft Sensor Technology in Refining and Chemical Units, Petrochemical Automation, Vol. 59 (2023) No. 2.

[4] Y.D. Su: Exploration and Application of Online Real-Time Optimization for Refining and Chemical Units, Petroleum Refinery Engineering, Vol. 53 (2023) No. 5, p.12-15.

[5] C.H. Yang, B. Sun, Y.G. Li, K.K. Huang and W.H. Gui: Cooperative Optimization and Intelligent Control of Complex Production Processes, Acta Automatica Sinica, Vol. 49 (2023) No. 3, p.528-539.

[6] Y. Jiang, S. Yin, J. Dong, et al.: A Review on Soft Sensors for Monitoring, Control, and Optimization of Industrial Processes, IEEE Sensors Journal, Vol. 21 (2021) No. 11, p.12868-12881.

[7] Y. Yu, M. Lee, C. Lee, et al.: Estimating APC Model Parameters for Dynamic Intervals Determined Using Change-Point Detection in Continuous Processes in the Petrochemical Industry, Processes, Vol. 11 (2023) No. 8, p.2229.

[8] Y.R. Li, C.J. Yang, H.W. Zhang and J.F. Li: Discussion on Key Technologies of Digital Twins for Process Industry, Acta Automatica Sinica, Vol. 47 (2021) No. 3, p.501-514.

ISSN: 2414-1895 DOI: 10.6919/ICJE.202605_12(5).0019

[9] P. Kumar, J.B. Rawlings and S.J. Wright: Industrial, Large-Scale Model Predictive Control with Structured Neural Networks, Computers & Chemical Engineering, Vol. 150 (2021), p.107291.

[10] Y. Xiong, X. Shi, Y. Ma, et al.: Optimization Design of Crude Oil Distillation Unit Using Bi-Level Surrogate Model, Frontiers in Control Engineering, Vol. 4 (2023), p.1162318.

[11] F. Fiedler, B. Karg, L. Luken, et al.: do-mpc: Towards FAIR Nonlinear and Robust Model Predictive Control, Control Engineering Practice, Vol. 140 (2023), p.105676.

[12] Y.S. Perera, D.A.A.C. Ratnaweera, C.H. Dasanayaka, et al.: The Role of Artificial Intelligence-Driven Soft Sensors in Advanced Sustainable Process Industries: A Critical Review, Engineering Applications of Artificial Intelligence, Vol. 121 (2023), p.105988.

.